Journal of Physics: Conference Series

PAPER • OPEN ACCESS

Development of diagnostic instrumentations for fuel cells based on consumer electronics

To cite this article: Thomas Dalberto *et al* 2023 *J. Phys.: Conf. Ser.* **2648** 012085

View the article online for updates and enhancements.

You may also like

- Pulse quenching based radiation-hardened by design technique for analog single-event transient mitigation on an operational amplifier in 28 nm bulk CMOS process
Jingtian Liu, Xinyu Xu, Qian Sun et al.

- Design analysis and experimental validation of relaxation oscillator-based circuit for R–C sensors
Mohamad Idris Wani, Sadan Saquib Khan, Benish Jan et al.

- Broadband, large scale acoustic energy harvesting via synthesized electrical load: II. Electrical load
Nathan M Monroe and Jeffrey H Lang

This content was downloaded from IP address 188.216.82.132 on 31/01/2024 at 00:25

Development of diagnostic instrumentations for fuel cells based on consumer electronics

***Thomas* Dalberto**[1], ***Francesco* Battistella**[1], ***Paolo* Colbertaldo**[1,*]

[1] Politecnico di Milano, Dipartimento di Energia, Via Lambruschini, 4a, 20156 Milano (MI), Italy

[*] Corresponding author: paolo.colbertaldo@mail.polimi.it

Abstract. The decarbonization process is pushing the energy sector into a transition towards clean energy vectors. In the hard-to-abate sectors, such as heavy-duty transport and industry, hydrogen can act as an energy carrier and a sector coupler. Key devices for hydrogen exploitation are fuel cells. Diagnostic is a crucial element for safety and efficiency during operation. This work regards the development process – from the conception to the validation and use – of an acquisition system made of consumer electronic components. By measuring differential voltage at high frequency, it enables to perform Electrochemical Impedance Spectroscopy (EIS). The system consists of an Arduino board running a self-developed circuit composed of an operational amplifier, an analog-to-digital converter, and a buffer memory. The system is designed to be expanded with multiple synchronized modules to monitor several cells at once. The module can be applied to a single cell or a group of cells (e.g., a stack) by tuning the operational amplifier. A dedicated software has also been developed, involving assembly language to achieve the required speed performance. The circuit has been validated using a function generator to apply sinusoids with frequencies between 100 Hz and 10 kHz and amplitudes of 10-500 mV (reflecting the EIS requirements on a single cell). An oscilloscope is used to double-check the generated signal. The results proved that the system features errors below 3% on amplitude and below 0.3% on frequency. Finally, the developed system has been tested against a commercial device performing EIS measurements. The obtained impedance values generally differ by less than 3% in the range of interest, while a few specific frequencies are affected by external disturbances.

1. Introduction

The ongoing process of decarbonization in response to climate change is driving the transition of the energy industry [1]. The use of renewable energy sources is a primary step in this process; however, their exploitation presents new challenges, such as intermittency, which call for solutions like energy storage or demand management [2]. Hydrogen is a promising energy carrier with a multiplicity of production pathways and multiple end uses. Fuel cells (FCs) are electrochemical devices that can efficiently convert hydrogen into electricity, without GHG or local pollutant emissions [3]. Thanks to the possibility of decoupling power and energy capacity, hydrogen systems are of high interest for seasonal storage. Given their high energy density, FCs are also particularly suitable for transport sector applications, mainly considering low-temperature technologies and in particular PEM (proton exchange membrane) fuel cell systems. Currently, the main drawback is the presence of precious metals (e.g., platinum) as catalyst in order to support dynamic behavior as typical of mobile uses, leading to high costs.

Content from this work may be used under the terms of the Creative Commons Attribution 3.0 licence. Any further distribution of this work must maintain attribution to the author(s) and the title of the work, journal citation and DOI.
Published under licence by IOP Publishing Ltd

Diagnostic is a crucial aspect regarding safety and efficiency during fuel cell operation. Therefore, it is important to have devices able to constantly monitor the performance, looking both at the stack and the single cells.

Among the diagnostic techniques, electrochemical impedance spectroscopy (EIS) is a useful tool since it is applicable online without interrupting the operation and can provide information on various origins of losses [4]. It is therefore used to analyze the components inside the cell, understanding if they have some issues, like poor membrane humidification or flooding, or to monitor their degradation. This type of test consists in the application of sinusoidal current perturbations at different frequencies to then measure the voltage responses of the stack or of a cell. The oscillation amplitude of the current perturbation is small with respect to the average current level to maintain the linear behavior. The typical value used is 5-10% I_{DC}. The impedance is then calculated by dividing the oscillation amplitude of the voltage response by the oscillation amplitude of the current response. The result is typically represented on a Nyquist plot which represent the inverse of the imaginary part of the impedance against its real part. Each point on the plot corresponds to the impedance at a certain frequency. A complete plot typically includes frequencies ranging from tens of kHz to several mHz [5] and allows to extract three resistances that can be related to various types of losses. On the market there are no offers for low-cost measuring devices specifically designed to measure the signal related to EIS tests of single cells of fuel cell stacks. The typical EIS devices embed all the functionality needed (i.e., perturbation of the cell and signal acquisition) and are usually designed to be able to perform EIS measurements also on other electrochemical devices, such as lithium-ion batteries. This leads to capabilities and performances exceeding those required by fuel cells, and results in more expensive devices.

In this context, this work focuses on the development of a high-speed acquisition system based on consumer electronics specifically designed for performing EIS on the single cells of fuel cell stacks. This system is designed to be modular with multiple modules that acquire the voltage of either a cell, a group of cells or the entire stack. The measurements of the modules are synchronized with each other, and this allows separate systems to perform the perturbation and the acquisition. The modularity of the system ensures its scalability, allowing to test it on a 1 kW fuel cell stack without losing the significance of the results since the scale is only related to the choice of the operational amplifier (further information on modularity in chapter 2). This system is applied to a fuel cell test rig developed in the Laboratory of Energy Conversion and Storage (LabX) for research and educational purposes. The test rig is improved integrating our EIS system. The current phase of the development focuses on the acquisition system, leaving an external instrument in charge of the generation of the perturbation. However, the method studied for synchronization of the systems is adaptable to other perturbation systems.

At the beginning of this article the methodology followed is presented. It begins by providing the necessary context in which the self-developed acquisition system is inserted. A description of the system is then presented followed by its usage and the process used for its validation. Following the methodology, another section is dedicated to the results obtained during the validation of the system in which the main outcomes derived from the experiments conducted are shown. Lastly, the article concludes by summarizing the key conclusions drawn from the work, emphasizing the significance and the implications of the findings.

2. Methods

This section describes the experimental apparatus to operate a fuel cell stack during the tests and the related equipment, which are used to validate the system. Then, the self-developed acquisition system is described in detail and the testing procedures are presented.

2.1. Description of the experimental apparatus

A test bench is used to operate a 1 kW water-cooled PEM fuel cell stack by PowerCell and to assess its performance. Tests are performed using the self-developed acquisition system. The test rig is meant to be also used in future fuel cell testing campaigns.

The test rig piping and instrumentation diagram (P&ID) is reported in Figure 1 and consists of the following five subsystems:

- **Gas supply system**. Three ball valves (HV901-1 - HV901-4) are used to manually switch on and off the gas feeds, and two three-way valves (HV901-5, HV901-6) are used to switch to N2 feed. Three BronkhorstTM mass flow controllers (FTC901) are used to control and measure the flow rates of H2, CH4, and air.
- **Humidification system**. A bubbler (601) on the cathode supply line provides a stream of saturated air at 80°C. This stream is mixed with fresh air from a bypass valve (HV601-1) that is regulated to control the relative humidity. The heat is provided by a 2-kW electric resistance. A second electric resistance, installed on the pipe connecting the bubbler to the fuel cell stack, prevents condensation downstream of the bubbler.
- **Electric load control**. A Chroma 63204A electronic load (902) dissipates up to 4 kWe and is used to impose the current to the fuel cell stack (901). The rated power is sufficient, considering that the employed fuel cell stack does not exceed 1.2 kWe. This device also performs real-time measurements of current and voltage across the stack and is used in conjunction with the self-developed acquisition system for the electrochemical impedance spectroscopy.
- **Thermal management system**. To heat up the fuel cell stack at startup, a closed circuit of water heated by a resistance (501) is used. To cool the fuel cell stack during operation, a small water-to-water heat exchanger (502) extracts heat from the circuit and transfers it to a continuous flow of cool water.
- **Pressure control system**. Two needle valves (HV901-8, HV901-9) mounted at the cathode and anode outlets generate a backpressure that pressurizes them, while maintaining the pressure difference within the allowed values. The valves are regulated manually according to pressure measurements at the fuel cell stack inlet from both a manometer and a transducer. The process of automating these components is ongoing, for which stepper motors have been sized and selected to drive the needle valves (implementation and testing ongoing).

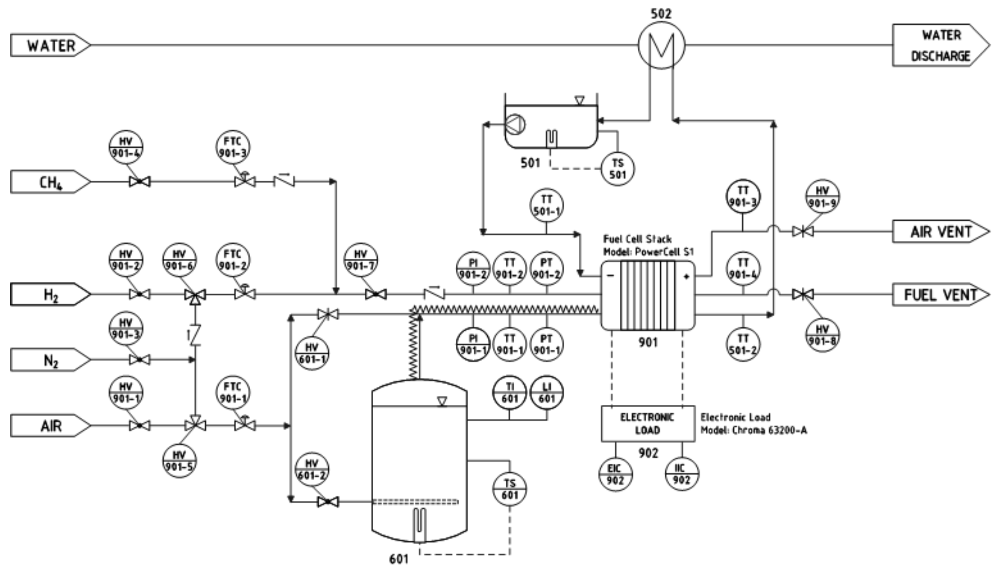

Figure 1. Piping and instrumentation diagram of the test rig.

The test rig is also equipped with temperature and pressure sensors. Their signals are processed by an Arduino MEGA board, which converts them to digital values that are then transmitted to the user interface running on the computer.

Table 1. Instrumentation installed on the apparatus for monitoring the operational conditions. Volume quantities are referred to normal conditions (0 °C, 101.325 kPa). F.S. stands for full scale, while R.V. for read value.

Parameter	Instrument	Range	Uncertainty
H_2 flow rates	Bronkhorst F201-CV	0 – 25 ln/min – hydrogen	0.2 %F.S. 0.5 %R.V.
Air flow rates	Bronkhorst F202-AV	0 – 110 ln/min – air	0.2 %F.S. 0.5 %R.V.
Pressure	BD|SENSORS DPM 331	0 – 2.5 bar	0.35 %F.S.
Voltage	Chroma 63204A	0 – 150 V	0.015 %F.S. 0.015 %R.V.
Current	Chroma 63204A	0 – 400 A	0.04 %F.S. 0.04 %R.V.
Temperature	K-type TC	0 – 1024 °C	0.3 °C

2.2. Development and implementation of an EIS measurement system

Starting from the Arduino MEGA used to acquire the sensors, we explore the possibility of exploiting its capabilities further by using it to perform Electrochemical Impedance Spectroscopy (EIS) measurements. To achieve this, the software is optimized a more advanced communication protocol is developed.

The software developed for the Arduino is written in C++ and utilizes low-level instructions to directly manipulate registers. This approach minimizes the number of instructions required to perform each task, resulting in faster program execution. The program follows a command-based architecture, which enables pseudo-dynamic code execution and facilitates a multi-tasking environment.

To transfer data from Arduino to the PC, a serial-based communication protocol is implemented. This protocol used commands as well and allows the PC to control various activities on the Arduino. For instance, it can trigger the high-speed acquisition system to perform EIS measurements, or it can require the last measurements available. The protocol is compatible with programming languages that support serial communication, including open-source solutions like Python.

In this project, the visualization and control software for the PC is built using LabVIEW®. The choice of LabVIEW® is motivated by the availability of numerous libraries at LabX.

This combination of the optimized software and the self-implemented command-based communication protocol enables the capability to perform multiple tasks concurrently on a single board. It ensures that each task operates at its maximum speed, thereby guaranteeing the responsiveness of the monitoring and control system. Furthermore, the developed communication protocol enables the data to be sent to the PC only upon request. This approach ensures that all the transmitted data are processed and not discarded, thereby enhancing the efficiency and reliability of the data transmission process.

Overall, this integrated system allows to acquire sensor data, perform EIS measurements, and efficiently communicate with the PC using a command-based communication protocol. The LabVIEW®-based software provides a user-friendly interface for visualization and control, making it a comprehensive solution for our monitoring and control needs.

The sinusoidal current perturbation required to perform EIS test is imposed using the test rig's Chroma 63204A electronic load, then the voltage across each cell is measured using the self-developed Arduino based system.

To correctly calculate the impedances of each cell, it is necessary to synchronize the measurements of both the cell voltage and the current flowing through each cell. The Chroma load measures the current and the stack voltage simultaneously, while the Arduino-based system measures the cell voltages and the stack voltage simultaneously. The measurements of cell voltages and current are synchronized by ensuring that the Fast Fourier Transforms of the stack voltage, measured by both systems at the same time, are in phase.

To overcome the sampling frequency limitations of the analog-to-digital converter (ADC) embedded in Arduino, an external ADC system. This external system is developed to achieve the required high-speed, synchronized measurements. On the Arduino that drives it, the C++ code must use the direct port manipulation instructions cited before to reach the required sampling frequency of 80 kHz needed to sample the high frequency signals involved in EIS tests.

The system consists of multiple modules. Each module is responsible for measuring the voltage difference of a single cell or stack. The main components forming the module are highlighted in Figure 2.

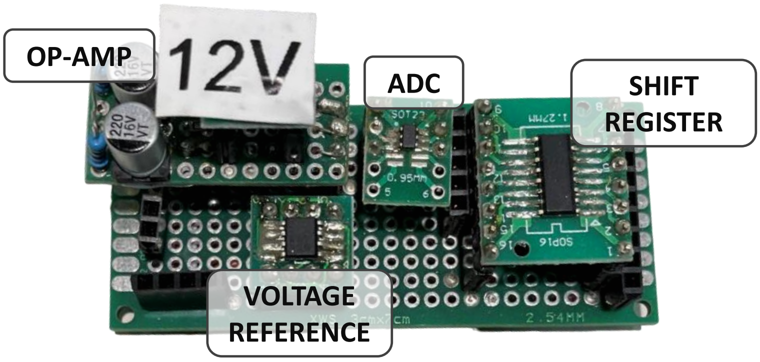

Figure 2. Module with labels to identify its main components.

The ADC performs the conversion of an analog signal to a digital one, which is transmitted in serial communication mode. The operational amplifier (op-amp) placed at the input of the ADC is used to configure the desired range of measurable signal amplitude and to provide a low impedance input to the ADC. It receives the signal of interest – which can be in the range 0-1.2 V for a single cell or 0-12 V for a 10-cell stack – and it outputs a proportional signal in the 0-5 V range, which is the optimal one to exploit the whole ADC resolution. This configuration of the ADC is specific to our setup of 10 cells; however, the same components can be tuned to test stacks with up to 25-30 cells in series (0-30 V) and any number of cells in parallel. The constraint depends on the op-amp maximum voltage of the stack module, therefore choosing one with a higher rated voltage just this module allows to increase the maximum number of cells in series. Even if such an operational amplifier could have lower accuracy, this does not impact the ability to measure the signals. The amplitude that need to be measured is in fact proportional to the number of cells, therefore it increases requiring lower accuracy. The shift register at the ADC output acts as a buffer temporarily storing the last measured value until Arduino is ready to read it. Moreover, it converts serial communication to a parallel one, allowing for a faster transfer of data into the Arduino memory. Lastly, the 5 V reference voltage is included to accurately interpret the digital signals obtained by the ADC.

2.3. *EIS signal and data processing*

The EIS test starts with the fuel cell stack in steady state at the operating point that needs to be tested. The frequencies sampled are equally spaced in the logarithmic scale and go from 10 kHz to 0.1 Hz. The amplitude is set to 40% of the steady state current (I_{DC}). This value is chosen based on the results from Ginger-Sanz *et al.* [6] and is based on THD minimization. The paper report that THD decreases up to 80% of I_{DC}; however, a more conservative 40% of I_{DC}, which is after the knee of the curve but is less risky for the stack, is chosen. The procedure used to acquire an EIS point is reported in Figure 3.

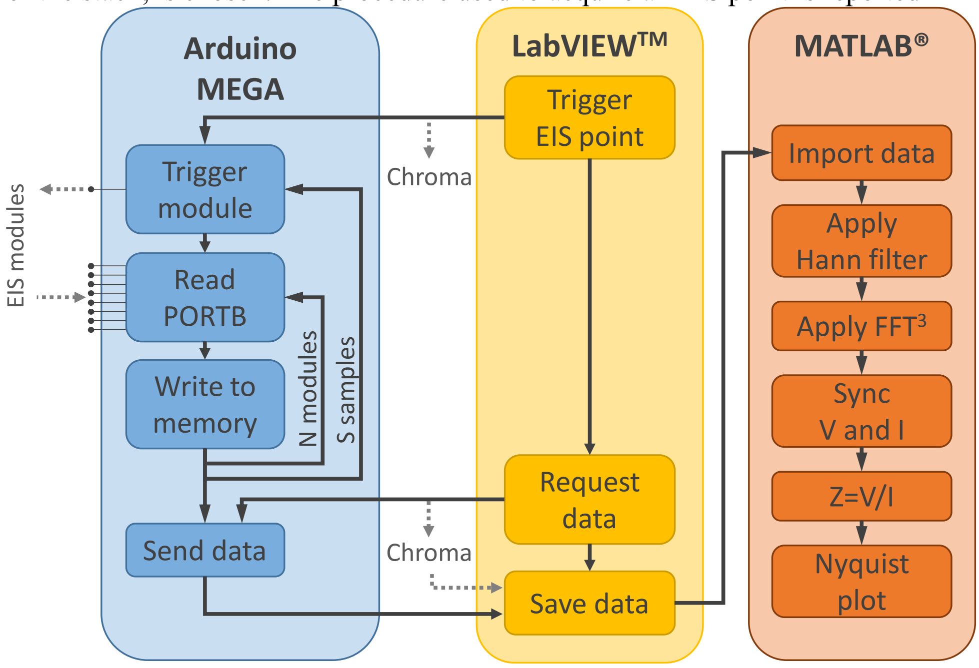

Figure 3. Diagram showing the main phases of the signal and data processing procedure.

It starts from the LabVIEW interface which sets the measurements parameters, such as the sampling frequency and the number of sample points, on both the Chroma electronic load and the Arduino. The electronic load then starts applying sinusoidal perturbation to the fuel cell stack. When everything is set, LabVIEW triggers the signal acquisitions on both the electronic load and on the Arduino. Focusing on what happens in the Arduino, once the trigger is received, it sends the starting signal to all the modules via a single wire which is connected to all of them. With the correct timings, it then asks the measured data to each module one at a time. When asked, the modules put the data on the bus connected to an Arduino port. Arduino can then read all the 8-bit data in a single operation and saves it in its memory before asking the next module for the data. Once the Arduino has all the samples in memory, it sends them to LabVIEW which saves them along with the data coming from Chroma. In a second time, those data are post-processed by a MATLAB script to extract useful information.

The post-processing script cycles on each perturbation frequency of a steady state operating point. For each of them it imports the Arduino table and the Chroma table. Frequency, amplitude, and phase of the fundamental component of the signals are obtained by means of the Fast Fourier Transform algorithm (FFT). The DC components are removed before applying the FFT. With the standard algorithm the phases would be biased by the discretization errors. To achieve higher precision, the corrected Fast Fourier Transform (cFFT) algorithm described by Biancacci et al. [7] is applied. The algorithm consists in performing a Hanning filtering of the signal before applying the FFT. In this way, the spectrums obtained have a particular property that makes the maximum identifiable on continuous frequency domain instead of the discrete one. To synchronize the measurements, the stack voltage phase is used as reference for the phases. Therefore, all the phasors of the Arduino and Chroma measurements are rotated by the phase of the stack voltage from their respective devices. The impedances are then calculated by dividing the voltage phasors by the current phasor. The impedances are then represented in a Nyquist plot by plotting the inverse of the imaginary part of each impedance against its real part. On the graph, each point of a curve is at a specific frequency and each curve is at a specific I_{DC}.

The quantitative result that can be extracted from the Nyquist plots are the high frequency resistance (HFR), the charge transfer resistance (RCT) and the mass transport resistance (RMT). The HFR is the impedance in correspondence to the point where the curve first crosses the real axis (around 3 kHz). The RCT is obtained by subtracting the HFR to the impedance in correspondence to the second crossing of the real axis. However, differently from the ideal case, in real measurements the curve does not really cross the axis, therefore the real point must be derived. In our case, the real part of the impedance in correspondence to the local minimum of the curve is chosen. Finally, the RMT is obtained by subtracting the RCT to the impedance in correspondence to the third and final crossing of the real axis.

2.4. EIS system validation procedures
Before validating the complete system, the following components of the designed circuit have been tested individually:

- Operational amplifier (op-amp). The tests show nearly perfect linearity (linear interpolation with R^2=1.0000) and the gain obtained matched the desired value of 4.030 with a small voltage offset of -0.036 V. The amplification factor is not influenced by the frequency in the range 1 Hz – 10 kHz, confirming that the bandwidth is sufficient for the EIS application.
- Analog-to-digital converter (ADC). A signal between 10 Hz and 10 kHz is generated using the TG1010A DDS function generator in conjunction with a WaveAce 234 oscilloscope, and it is then sampled by the ADC at a sampling frequency 10 times larger than the signal frequency. The initial test proved that the procedure for controlling the ADC works and that with a MATLAB™ script it is possible to reconstruct each signal.

After those preliminary evaluations, some tests have been performed on the complete modules to verify the correct interaction between the components and to validate the circuit. The minimum working setup consists of a module to measure the cell voltage (cell digitizer module) and a second module to measure the stack voltage (stack digitizer). The two differ by the configured gain on the op-amp. This setup is the one implemented due to the effort required to produce nine additional, identical modules to perform the measurement of all the cells simultaneously. However, the tests are performed simulating the presence of 11 modules (one per cell and one for the whole stack) by repeatedly asking the same measurement data to the two modules alternatively, to demonstrate the possibility to operate 11 of them simultaneously.

In the first test, a signal generated by a TG1010A DDS function generator is measured using the designed circuit. A WaveAce 234 oscilloscope is used to check the real signal applied. This test is applied to both the cell and stack digitizers. In the second test, instead, the stack digitizer module and the Chroma load, considered superior, perform the same EIS measurement on the real fuel cell stack and their results are compared.

3. EIS system validation results
To validate the EIS acquisition system, known signals are measured, and the reconstructed signals obtained are compared with the imposed ones. The comparison is made in terms of relative difference of amplitude and frequency (**Error! Reference source not found.**) obtained by the FFT with respect to those measured by the oscilloscope.

 2648 (2023) 012085 doi:10.1088/1742-6596/2648/1/012085

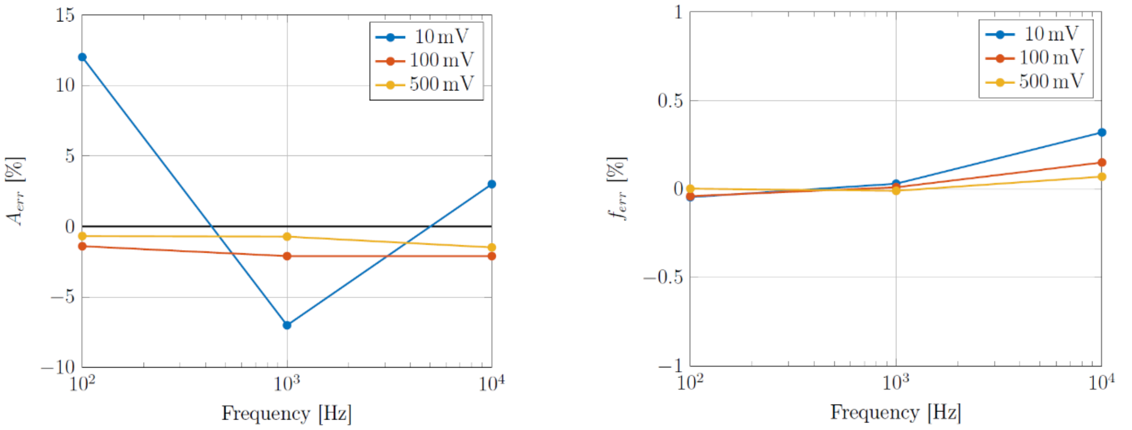

Figure 4. Error of the voltage amplitude (left) and of the frequency (right) estimated via FFT of cell digitizer result with respect to the imposed signal, for different signal peak to peak amplitudes.

For signal amplitude greater than 100 mV the error obtained is below 3% up to 10 kHz. Decreasing the amplitude of the signal, the error increases, exceeding 10% when the V_{PP} reaches 10 mV. This is due to the system resolution: 8-bit ADC resolution means that 256 voltage levels between 0 and 5V can be represented leading to discrete intervals of $5000/256 = 19.53\, mV$. The amplification factor is 4.03, therefore the step before the amplification is $19.53/4.03 = 4.846\, mV$. With this resolution, the 10 mV amplitude can only be represented by 2 or 3 levels.

The signals are oversampled, meaning the sample frequency is more than twice the signal frequency, in this case 10 times, and this increases the resolution by averaging the measurements [8]. Still, with just 2 or 3 amplitude levels representing the signal, it is difficult to estimate the correct signal amplitude.

Another type of validation, performed only on the stack module, consists in performing a real EIS measurement on the fuel cell stack with both the Chroma and the own-developed stack digitizer under validation. The modulus of the impedances obtained at each frequency from both the systems are then compared in terms of percentage difference (Figure 5).

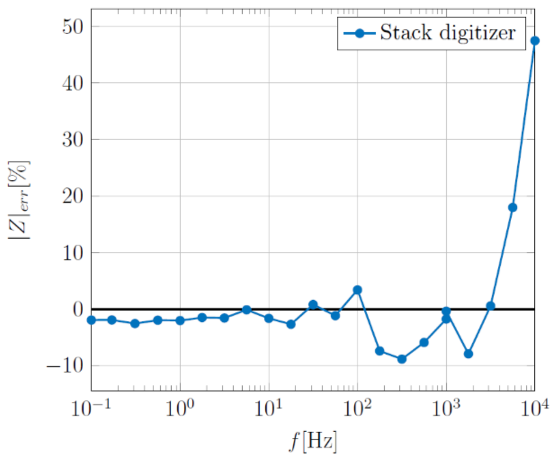

Figure 5. Error of the impedance modulus (estimated via FFT) resulting from the stack digitizer with respect the Chroma internal digitizer.

The results from the two systems are quite in accordance, especially for frequency that are multiple of 10 where the deviation stays below 5% in various tests performed. For frequencies between 100 Hz and 1 kHz the error is around 10%, and it is supposed that this can be due to some effect of the difference in the discrete representations inside the Chroma and Arduino, however this behavior has not been investigated further since it does not have a significant impact on the estimations of the resistances.

At 10 kHz the deviation reaches almost 50%. The cause of this deviation has not been identified since the curve reconstruction with the function generation is good at similar frequency and amplitude. For the 3 kHz measurement there is good accordance between the systems, and from the Nyquist plots presented in Figure 6, it can be observed that this frequency, is enough to cross the real axis and therefore identify the high frequency resistance.

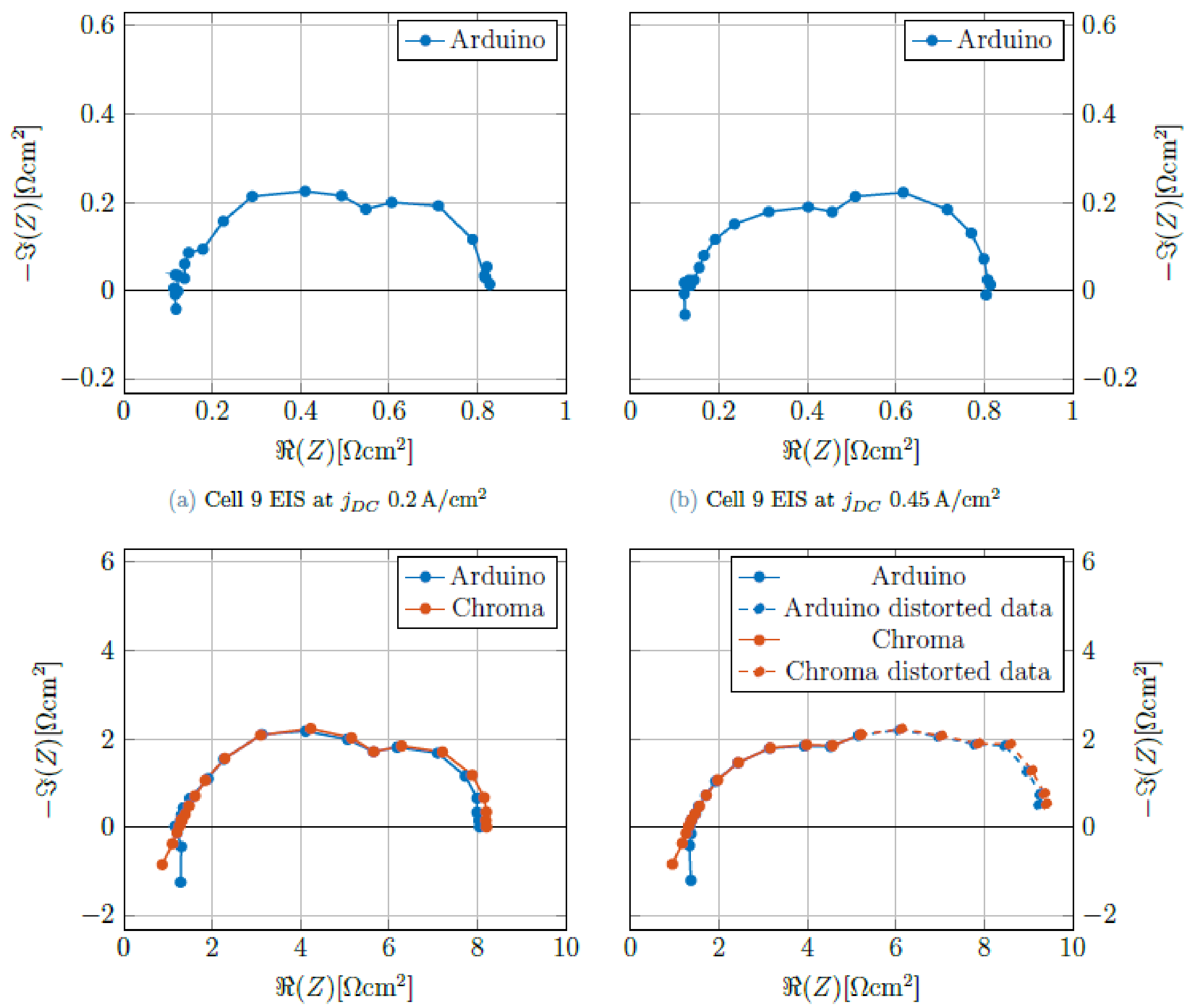

(a) Cell 9 EIS at j_{DC} 0.2 A/cm^2
(b) Cell 9 EIS at j_{DC} 0.45 A/cm^2
(c) Stack EIS at j_{DC} 0.2 A/cm^2
(d) Stack EIS at j_{DC} 0.45 A/cm^2

Figure 6. Nyquist plots of cell 9 (a and b) and of the entire stack (c and d), as obtained with the self-developed acquisition system and with the Chroma electronic load.

4. Conclusions

In this work, an acquisition system for EIS applications based on consumer electronics has been developed, built, and validated. To perform the study, a test rig for fuel cell stacks has been used. Results have been obtained on a 10-cell stack (nominal power 1 kW), but the validity of the solution is general thanks to the intrinsic modularity, given the presence of an adequate op-amp.

The self-developed system works with less than 3% error on amplitude and less than 0.3% error on frequency when compared with an oscilloscope. With respect to a commercial device, the obtained stack impedance generally differs by less than 5% in the range of interest for the EIS measurement, with deviations reaching 10% for few specific frequencies due to external disturbances. Moreover, the system theoretically proved to be able to perform the EIS of up to ten cells at the same time, just by repeating the single-cell module. Their implementation will confirm this capability.

To sum up, it is concluded that consumer-electronics with proper tuning can be exploited with results comparable to scientific instruments in EIS applications. This has some significant implications. First, it highlights the potential for increasing accessibility and affordability of EIS in fuel cell research, allowing researchers to perform EIS experiments even without access to expensive instruments. This can lead to greater advancement in the field of EIS and, more in general, of fuel cells. Secondly, the finding emphasizes the integration capabilities of consumer-electronics devices which are multifunctional and can integrate with various sensors and control strategies. By also integrating EIS measurements, data collection, processing, and sharing can be facilitated.

Further improvements could be attained by switching to the use of an actual memory instead of the shift register to increase sampling frequency and to remove the need for limiting ADC resolution to 8 bits. As a future research topic, it could be tested whether applying a step perturbation it is possible to retrieve the same EIS information analyzing different frequency components superimposed in the response.

References

[1] IRENA. World Energy Transitions Outlook 2022, 2022. URL: https://www.irena.org/Digital-Report/World-Energy-Transitions-Outlook-2022. [Last Accessed: May 19th 2023].

[2] A. Headley, D. Copp. Energy storage sizing for grid compatibility of intermittent renewable resources: A California case study. Energy, 198:117310, 2020. doi: https://doi.org/10.1016/j.energy.2020.117310.

[3] F. Barbir. PEM fuel cells: Theory and practice. PEM Fuel Cells: Theory and Practice, pages 1–518, 2012. doi: https://doi.org/10.1016/c2011-0-06706-6.

[4] X. Zhang, T. Zhang, H. Chen, and Y. Cao. A review of online electrochemical diagnostic methods of on-board proton exchange membrane fuel cells. Applied Energy, 286:116481, 3 2021. doi: https://doi.org/10.1016/j.apenergy.2021.116481.

[5] A. Lasia. Electrochemical impedance spectroscopy and its applications. Modern Aspects of Electrochemistry, pages 143–248, 2002. doi: https://doi.org/10.1007/0-306-46916-2_2.

[6] J. J. Giner-Sanz, E. M. Ortega, and V. Pérez-Herranz. Optimization of the perturbation amplitude for impedance measurements in a commercial PEM fuel cell using total harmonic distortion. Fuel Cells, 16:469–479, 2016. doi: https://doi.org/10.1002/fuce.201500141.

[7] N. Biancacci, M. Giovannozzi, F. Schmidt, E. Métral, Y. Papaphilippou, B. Salvant, and R. Tomás. FFT corrections for tune measurements, 2011. URL: https://indico.cern.ch/event/132526/contributions/128902/attachments/99707/142376/Meeting1-06-11_FFT_corrections_for_tune_measurements.pdf. [Last Accessed: May 18th 2023].

[8] M. Pachchigar. Increase dynamic range of SAR ADCs using oversampling | analog devices, 2015. URL: https://www.analog.com/en/technical-articles/increase-dynamic-range-of-sar-adcs-using-oversampling.html. [Last Accessed: May 18th 2023].